

Improved parameterization of the SDWBA for estimating krill target strength

Stéphane G. Conti and David A. Demer

Conti, S. G., and Demer, D. A. 2006. Improved parameterization of the SDWBA for estimating krill target strength. — ICES Journal of Marine Science, 63: 928–935.

Recently, a Stochastic Distorted Wave Born Approximation (SDWBA) model was proposed to improve target strength (TS) estimates for Antarctic krill, *Euphausia superba*. The krill shape is modelled by a collection of cylinders, and total sound scatter is estimated by semi-coherent summation of scatter from each element. The SDWBA model was evaluated with a generic krill shape comprising 14 cylinders and a phase variability of $\sqrt{2}/2$ radians, and predictions were validated with empirical TS and total TS data at 120 kHz, and over a broad bandwidth, respectively. For general application, parameterization of the SDWBA model is improved to account explicitly for dependence among four of the model parameters: standard length of krill, number of cylinders used to describe its shape, amplitude of inter-element phase variability, and acoustic frequency. The model improvements are demonstrated, and the uncertainty in orientation distribution of krill beneath survey vessels and its ramifications on krill biomass estimates are highlighted.

© 2006 International Council for the Exploration of the Sea. Published by Elsevier Ltd. All rights reserved.

Keywords: Antarctic krill, backscattering cross-section, SDWBA model, sensitivity, target strength.

Received 13 September 2005; accepted 23 February 2006.

S. G. Conti and D. A. Demer: Southwest Fisheries Science Center, 8604 La Jolla Shores Drive, La Jolla, CA 92037, USA. Correspondence to S. G. Conti: tel: +1 858 534 7792; fax: +1 858 546 5652; e-mail: sconti@ucsd.edu.

Introduction

Antarctic krill, *Euphausia superba*, are the basis of the ecosystem in the Southern Ocean and the target of a large international fishery. To support management strategies for the resource, surveys of krill dispersion and abundance are conducted using multi-frequency echosounders. Estimates of krill target strength (TS) are used to convert the total backscattered acoustic energy attributed to krill into an estimate of krill abundance (Hewitt *et al.*, 2002). The accuracy of the biomass estimate is directly proportional to the accuracy of the TS estimate (Demer, 2004). Krill TS depends on the animal size, shape, and morphology, and the acoustic wavelength and angle of incidence.

To account for the many factors influencing krill TS, McGehee *et al.* (1998) proposed a physics-based model based on the distorted-wave Born approximation (DWBA; Morse and Ingard, 1968). The krill body is idealized by a string of discrete bent cylinders. Krill TS is estimated from the coherent summation of scattering from each of the cylinders. This model was validated for dorsal aspect, on the main scattering lobe, at 120 kHz, from measurements with a live krill (McGehee *et al.*, 1998). However, there were large discrepancies between the model and data off the main axis.

Demer and Conti (2003a) introduced the Stochastic Distorted Wave Born Approximation (SDWBA) to explain the discrepancies between measurement and theory. Relative to the DWBA, the SDWBA accounts for the flexure and complexity of the krill body by incorporating a phase variability term φ_j between the scattering form functions of each individual cylinder j of the body. Thus, the SDWBA provides a more realistic prediction of field measurements of sound scattering from krill. The SDWBA model was validated with the McGehee *et al.* (1998) TS measurements at 120 kHz (Demer and Conti, 2003a), and total target strength (TTS) measurements of Antarctic krill (Demer and Conti, 2003b) and northern krill (Conti *et al.*, 2005).

For all these studies, the SDWBA model was evaluated using a generic krill shape (Figure 1), $N_0 = 14$ cylinders, and a standard deviation of the phase variability $\text{s.d.}_{\varphi_0} = \sqrt{2}/2$ radians. The selection of these parameters followed the shape and N_0 parameters used in McGehee *et al.* (1998), and an empirical determination of s.d._{φ_0} , respectively. N , s.d._{φ} , f , and the krill standard length L are dependent in their effects on the SDWBA predictions.

To illustrate these dependences, the SDWBA was solved with the generic krill shape (McGehee *et al.*, 1998), fattened by 40% (Demer and Conti, 2003a). The s.d._{φ} was increased from $\text{s.d.}_{\varphi_0}/10$ to s.d._{φ_0} , in $\text{s.d.}_{\varphi_0}/10$ intervals, with

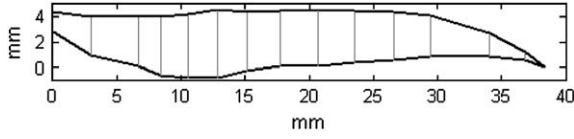


Figure 1. Shape of the generic $L_0 = 38.35$ mm krill defined with $N_0 = 14$ cylinders in the X - Z plane.

$f = 100$ and 200 kHz and $N = 14$ and 22 , respectively (Figure 2). At 100 and 200 kHz, the theoretical predictions remain the same on the main scattering lobe, independently of s.d. $_{\varphi}$. Off the main axis, however, the TS predictions increase with increasing s.d. $_{\varphi}$. As the maximum value of s.d. $_{\varphi} = \sqrt{2}/2$ radians was determined from the McGehee *et al.* (1998) measurements made at 120 kHz, the SDWBA predictions at 100 kHz with the maximum s.d. $_{\varphi}$ can be viewed as the benchmark. In contrast, at 200 kHz, the theoretical predictions show unrealistic values off the main axis as s.d. $_{\varphi}$ becomes too large. Remarkably, maximum TS shifts from the main scattering lobe. Next, f and s.d. $_{\varphi}$ were held constant and N was modulated from 14 to 28 in increments of 2 (Figure 3). The SDWBA predictions are only stable if N is large relative to the ratio of fish length to wavelength, to ensure an accurate representation of the body in regard to wavelength.

These examples clearly demonstrate the need to adjust s.d. $_{\varphi}$ and N vs. f and L via better parameterization of the SDWBA. Here, the SDWBA model is improved to account explicitly for the interdependence of these factors.

Methods

The calculations for SDWBA have been well described (McGehee *et al.*, 1998; Demer and Conti, 2003a). The formulation is repeated here to provide a convenient reference for the subsequent model derivations.

Krill is approximated by N discretized-bent cylinders of various radii a_j . In that case, the backscattering form function for the cylinder j and incident angle θ is

$$f_{bs_j}(\theta) = \frac{k_1}{4} \int [\gamma_{\kappa} - \gamma_{\rho}] \exp(-2i\vec{k}_i \cdot \vec{r}_0) \times \frac{a_j J_1(2k_2 a_j \cos \beta_{\text{tilt}})}{\cos \beta_{\text{tilt}}} dr_0, \quad (1)$$

where $\gamma_{\kappa} = (\rho_1 c_1^2 / \rho_2 c_2^2) - 1$, $\gamma_{\rho} = (\rho_2 - \rho_1) / \rho_2$, the subscript 1 denotes the ambient seawater and 2 the krill. J_1 is the Bessel function of first kind of order 1, \vec{r}_0 the position vector,

$$\vec{k}_i = k_1 \begin{bmatrix} \sin \theta \\ 0 \\ \cos \theta \end{bmatrix}$$

the incidence wave vector, and β_{tilt} the angle between the cylinder and the central axis of the body. The form function for the SDWBA is obtained by summing the components from each cylinder with a different random phase φ_j :

$$f_{bs}(\theta) = \sum_{j=1}^N f_{bs_j}(\theta) \exp(i\varphi_j). \quad (2)$$

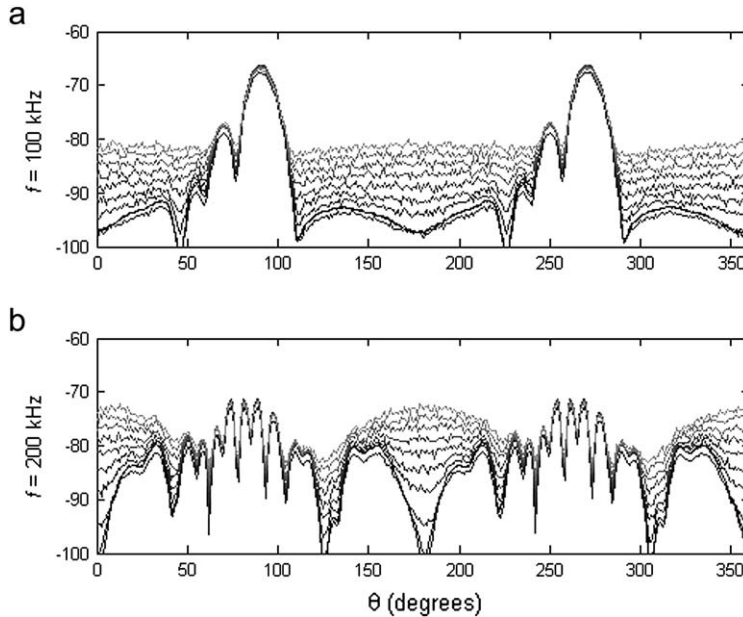


Figure 2. Target strength in dB estimated by the SDWBA model using a generic krill shape, $L_0 = 38.35$ mm, $f = 100$ kHz (a) and 200 kHz (b), with $N = 14$ and 22 , respectively. The standard deviation of the phase variability s.d. $_{\varphi}$ is stepped by $x\sqrt{2}/2$ radians, where x varies from 0.1 to 1.0 by 0.1 (from dark to light). The dorsal aspect corresponds to a 90° incident angle θ .

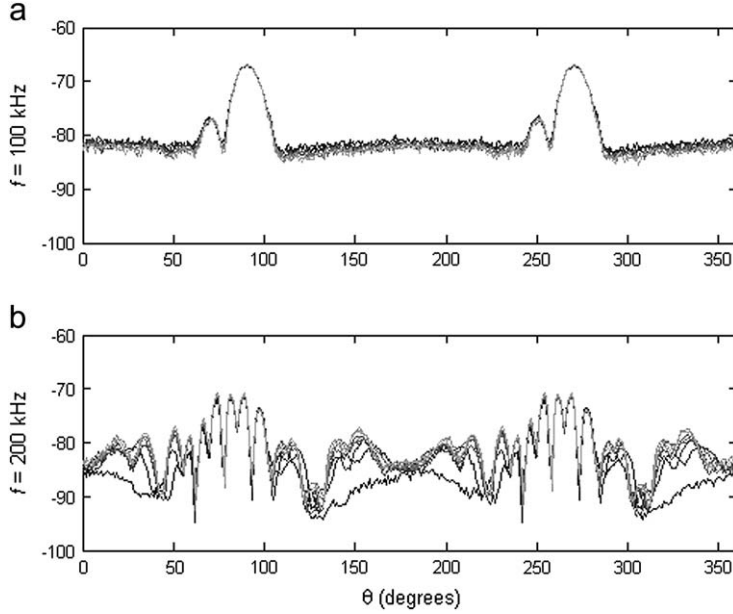


Figure 3. Target strength in dB estimated by the SDWBA model using a generic krill shape, $L_0 = 38.35$ mm, $f = 100$ kHz (a) and 200 kHz (b), with $\text{s.d.}_{\varphi_0} = \sqrt{2}/2$ (a), and $\sqrt{2}/4$ (b), respectively. The number of cylinders N varies from 14 to 28 in increments of 2 (from dark to light). The dorsal aspect corresponds to a 90° incident angle θ .

The phase variability φ_j is obtained from a Gaussian distribution centred on 0, with standard deviation s.d._{φ} , for each cylinder j along the body. Finally, the backscattering cross-section $\sigma_{\text{bs}}(\theta)$ is obtained from the average of multiple realizations of the ensembles of phase φ_j :

$$\sigma_{\text{bs}}(\theta) = \langle |f_{\text{bs}}(\theta)|^2 \rangle_{\varphi}, \quad (3)$$

and

$$\text{TS}(\theta) = 10 \log_{10}(\sigma_{\text{bs}}(\theta)). \quad (4)$$

The generic krill shape was defined by McGehee *et al.* (1998, standard length $L_0 = 38.35$ mm). The width of the generic shape was increased by 40% in Demer and Conti (2003a), because freshly caught krill were fatter than the starved animals measured in McGehee *et al.* (Figure 1). At $f_0 = 120$ kHz, and with $N_0 = 14$ cylinders, s.d._{φ_0} was estimated to be $\sqrt{2}/2$ radians from comparison of the SDWBA predictions with the experimental measurements. The factors N , s.d._{φ} , f , and L are dependent in their effects on the SDWBA results; the model will be improved if it can account explicitly for the interdependence of these factors.

To ensure generalized utility of the SDWBA, s.d._{φ} must be expressed as a function of f , N , and L . First, as the flexure and complexity of the body are frequency-independent, the product $\text{s.d.}_{\varphi}(f)f$ must be constant,

$$\text{s.d.}_{\varphi}(f)f = \text{s.d.}_{\varphi_0}f_0. \quad (5)$$

Also, if the frequency f or the body length L is modified, then N must be adjusted so that the spatial resolution of the body of the krill remains constant relative to wavelength λ . The ratio between wavelength λ and the length of each individual cylinder must remain constant:

$$\frac{L}{N\lambda} = \frac{L_0}{N_0\lambda_0}, \quad (6)$$

or

$$\frac{Lf}{N} = \frac{L_0f_0}{N_0}. \quad (7)$$

From Equations (5) and (7),

$$N(f, L) = N_0 \frac{fL}{f_0L_0}, \quad (8)$$

and

$$\text{s.d.}_{\varphi}(f, L) = \text{s.d.}_{\varphi_0} \frac{N_0L}{N(f, L)L_0}. \quad (9)$$

Thus, s.d._{φ} and N can be adjusted to the desired L and f . For example, TS was estimated at $f = 120, 200, 300,$ and 400 kHz by solving the SDWBA with a generic 40% fat krill shape, $L = L_0$, and adjusting N and s.d._{φ} according to

Table 1. Values of the number of cylinders N and the standard deviation of the phase variability $s.d._\varphi$ for the generic fat krill shape at frequencies f of 120, 200, 300, and 400 kHz. The standard parameters N_0 and $s.d._{\varphi_0}$ were obtained from comparisons of the model with the measurements at 120 kHz from McGehee *et al.* (1998).

f (kHz)	120 (f_0)	200	300	400
N	14 (N_0)	24	35	47
$s.d._\varphi$ (radians)	$0.5\sqrt{2}(s.d._{\varphi_0})$	$0.3\sqrt{2}$	$0.2\sqrt{2}$	$0.15\sqrt{2}$

Equations (8) and (9) with $N_0 = 14$ and $s.d._{\varphi_0} = \sqrt{2}/2$ radians. The values of the parameters with frequency are summarized in Table 1.

Results and discussion

By applying the improved parameterization to the SDWBA model, there are no unrealistic off-axis lobes in the TS predictions (Figure 4). Correct adjustment of $s.d._\varphi$ provides a realistically stable and frequency-independent plateau, ca. -80 dB, off the main scattering lobe.

Accurate application of the generalized SDWBA model still requires accurate characterization of the many parameters, particularly the orientation distribution of krill beneath a survey vessel (Demer and Conti, 2005), and density and sound-speed contrasts (g and h ; Foote *et al.*, 1990; Chu and Wiebe, 2005). The implications of TS modelling

with SDWBA can be illustrated using the distribution of krill lengths and volume-backscattering strength measurements at 120 and 38 kHz ($SV_{120 \text{ kHz}} - SV_{38 \text{ kHz}}$) from an international survey of krill in the Scotia Sea (Hewitt *et al.*, 2002). The survey is subdivided in three geographic regions (cluster C1, C2, and C3), according to the length distributions of krill. The SDWBA model was inverted in a least-squares sense to estimate an *in situ* distribution of orientations for each cluster individually, and for all clusters weighted by surveyed area or by krill net-catches. The mean and standard deviation of the normal distributions of orientation for the least-squares estimate ranged from 0° to 25° and 1° to 30° , respectively, by 1° steps. The distributions of orientations for clusters 1, 2, and 3 are estimated to normal distributions with a mean of 9° , 4° , and 3° and a standard deviation of 1° , 2° , and 1° , respectively (Figure 5a–c). For all clusters weighted by surveyed cluster area or krill catch demographics, the distributions of orientations are estimated to $N(4^\circ, 2^\circ)$ and $N(11^\circ, 4^\circ)$, respectively (Figure 6a, b). This last result should be compared with the previously published orientations of distributions from Kils (1981), Endo (1993), or Demer and Conti (2005). With the same data used by Demer and Conti (2005), but considering only the least-square criteria, an $N(11^\circ, 4^\circ)$ distribution of orientations gave a better fit to the data than the previously reported $N(15^\circ, 5^\circ)$ (Demer and Conti, 2005), or those

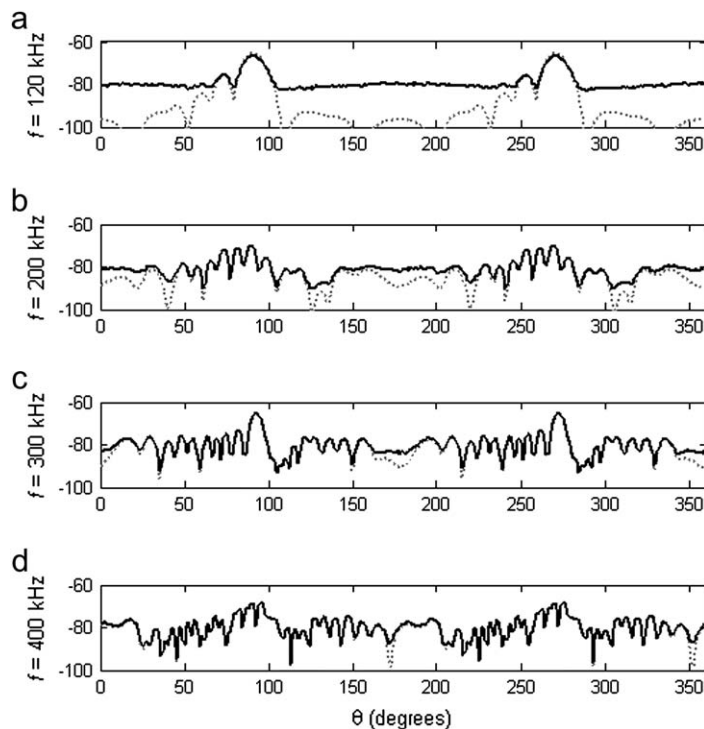


Figure 4. Target strength in dB estimated by the DWBA model (dotted lines) and the SDWBA model (solid lines) using a generic krill shape, $L_0 = 38.35$ mm, $f = 120$ kHz (a), 200 kHz (b), 300 kHz (c), and 400 kHz (d), and varying N and $s.d._\varphi$ according to Equations (8) and (9) (Table 1). The dorsal aspect corresponds to a 90° incident angle θ .

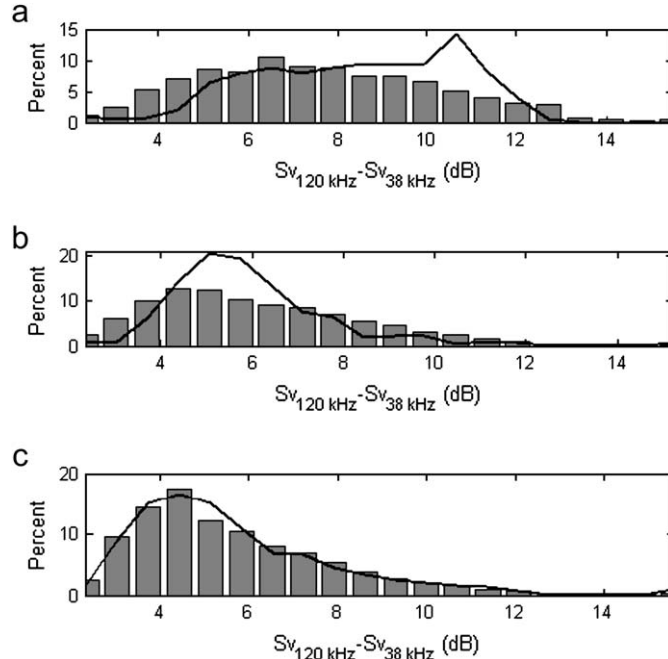


Figure 5. The differences in volume-backscattering strengths (S_v) attributed to krill at 120 and 38 kHz measured from RV “Yuzhmorgeologiya” during the CCAMLR 2000 survey for each cluster (grey bars), compared with predictions from the SDWBA model solved with the CCAMLR 2000 krill-length frequency distribution and the following krill-orientation distributions: (a) cluster 1, $N(9^\circ, 1^\circ)$; (b) cluster 2, $N(4^\circ, 2^\circ)$; (c) cluster 3, $N(3^\circ, 1^\circ)$.

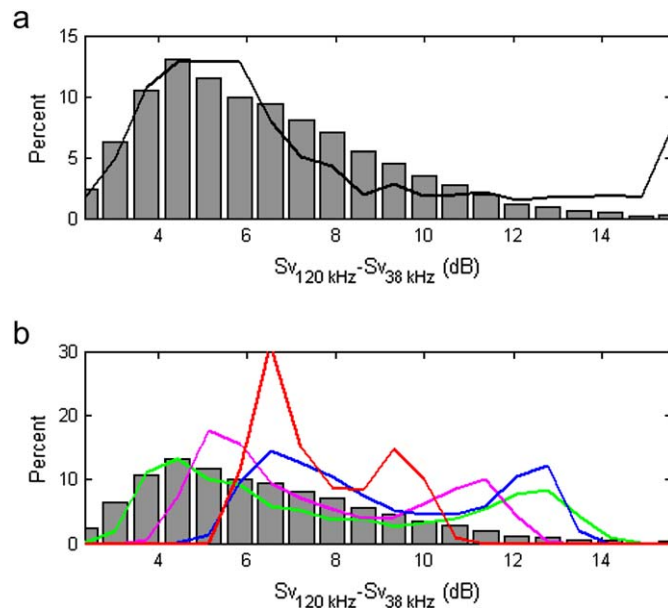


Figure 6. The differences in volume-backscattering strengths (S_v) attributed to krill at 120 and 38 kHz measured from RV “Yuzhmorgeologiya” during the CCAMLR 2000 survey for all clusters weighted (a) by surveyed cluster area, or (b) by krill catch demographics (grey bars), compared with predictions from the SDWBA model solved with the CCAMLR 2000 krill-length frequency distribution and the following krill-orientation distributions: (a) $N(4^\circ, 2^\circ)$ and (b) $N(11^\circ, 4^\circ)$ (green). On (b) also are the predictions from the SDWBA model solved with orientation distributions from the literature: Demer and Conti (2005) ($N(15^\circ, 5^\circ)$, magenta); Kils (1981) ($N(45.3^\circ, 30.4^\circ)$, blue); and Endo (1993) ($N(45.6^\circ, 19.6^\circ)$, red).

Table 2. Coefficients and reference length (L_0) for the simplified SDWBA model of krill TS (Equation (10)), averaged over krill-orientation distributions of $\theta = N(11^\circ, 4^\circ)$, $N(9^\circ, 1^\circ)$, $N(4^\circ, 2^\circ)$, $N(3^\circ, 1^\circ)$, and $N(15^\circ, 5^\circ)$ distributions of krill orientations. Exponential notation ($\times 10^x$) is denoted by “eC”. The coefficients can be used for values of kL smaller than 200, with a δ mean error in decibels between the exact and the simplified SDWBA.

	$N(11^\circ, 4^\circ)$	$N(9^\circ, 1^\circ)$	$N(4^\circ, 2^\circ)$	$N(3^\circ, 1^\circ)$	$N(15^\circ, 5^\circ)$
<i>A</i>	6.64558746	9.53903598	17.5946741	17.0371316	-2.49905225
<i>B</i>	0.127909076	0.150232083	0.148678743	0.141071237	8.61853594e-2
<i>C</i>	0.446318146	0.481046118	0.477644682	0.465029722	0.416196860
<i>D</i>	-1.19209591e-11	2.38762984e-11	-2.44990441e-11	-3.62685024e-11	-1.37800143e-11
<i>E</i>	7.42324712e-9	-1.42987306e-8	1.49734855e-8	2.21571676e-8	8.64846875e-9
<i>F</i>	-1.73916236e-6	3.26836233e-6	-3.47391012e-6	-5.14754726e-6	-2.06625975e-6
<i>G</i>	1.86327198e-4	-3.55716215e-4	3.73150405e-4	5.58016486e-4	2.31748271e-4
<i>H</i>	-8.67465215e-3	1.84888058e-2	-1.76600710e-2	-2.71990801e-2	-1.19024092e-2
<i>I</i>	0.132140873	-0.367180096	0.292424038	0.461708148	0.201695777
<i>J</i>	-81.3379373	-81.1053992	-84.7167863	-84.4621760	-76.6647548
L_0 (m)	38.35e-003	38.35e-003	38.35e-003	38.35e-003	38.35e-003
δ (dB)	2.18	1.48	1.00	0.95	3.23

reported by Kils (1981) or Endo (1993) (Figure 6b). However, two modes are predicted for the $Sv_{120\text{ kHz}} - Sv_{38\text{ kHz}}$ differences. For $N(15^\circ, 5^\circ)$, both modes fit within the empirical distribution, but the empirical distribution is broader. In contrast, as the mean and the standard deviation of the orientation distributions decrease (e.g. for $N(11^\circ, 4^\circ)$ and

$N(4^\circ, 2^\circ)$), the predicted upper modes are not supported by the empirical data. Therefore, the last two distributions are also equivocal. One possible explanation, however, is that this second mode at higher $Sv_{120\text{ kHz}} - Sv_{38\text{ kHz}}$ differences would correspond to small krill not detected at 38 kHz.

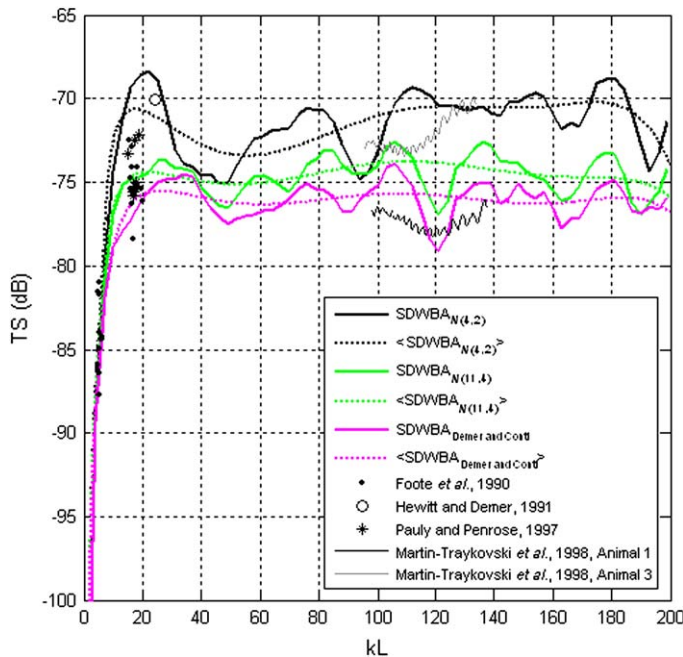


Figure 7. Target strengths TS for a 38.35 mm long generic krill predicted by the SDWBA (solid lines) and the simplified SDWBA (dotted lines), for the $N(4^\circ, 2^\circ)$ (black), $N(11^\circ, 4^\circ)$ (green), and $N(15^\circ, 5^\circ)$ (Demer and Conti, 2005; magenta) distributions of animal orientation. Also plotted are krill TS data measured *in situ* with a split-beam, 120-kHz echosounder (Hewitt and Demer, 1991) inferred from volume backscatter at 38 and 120 kHz from aggregations of krill (Foote *et al.*, 1990), measured from many individual live krill in a tank at 120 kHz (Pauly and Penrose, 1998), and measured from two live animals over a broad bandwidth (425–600 kHz; Martin-Traykovski *et al.*, 1998), and averaged over the $N(11^\circ, 4^\circ)$ orientation distribution.

Recognizing uncertainty in the orientation distribution, Demer and Conti (2005) provided a simplified SDWBA model for convenient estimation of Antarctic krill TS:

$$\text{TS(kL)} = A \left[\frac{\log_{10}(BkL)}{BkL} \right]^C + D(kL)^6 + E(kL)^5 + F(kL)^4 + G(kL)^3 + H(kL)^2 + I(kL) + J + 20 \log_{10} \left(\frac{L}{L_0} \right). \quad (10)$$

Here, we provide new coefficients for this simplified model which account for the generalized parameters in Equations (8) and (9), and a larger range of kL, for $\theta = N(11^\circ, 4^\circ)$, $N(9^\circ, 1^\circ)$, $N(4^\circ, 2^\circ)$, $N(3^\circ, 1^\circ)$, and $N(15^\circ, 5^\circ)$ (Table 2). The new simplified SDWBA can be evaluated for higher values of kL up to 200, compared with 50 in Demer and Conti (2005). The associated errors δ for the simplified SDWBA are about 1–3 dB, depending on the orientation distribution. The mean error can be reduced by increasing the order of the polynomial for the simplified SDWBA (Figure 7), but here the order of the polynomial was chosen according to Demer and Conti (2005). A comparison of krill TS vs. kL with $\theta = N(11^\circ, 4^\circ)$ shows good agreement with empirical data reported in the literature (Figure 7). Note, however, that the empirical TS data do not include measurements of krill

orientation, except for those from Martin-Traykovski *et al.* (1998). SDWBA predictions of krill TS averaged over $N(4^\circ, 2^\circ)$ and $N(15^\circ, 5^\circ)$ are, respectively, above and below those averaged with $N(11^\circ, 4^\circ)$. All three of these distributions of orientations suggest that krill are swimming fast beneath the surveying vessel (Kils, 1981).

Finally, the application of the SDWBA using $N(11^\circ, 4^\circ)$ results in a krill biomass estimate nearly three times the previous estimate made using the Greene *et al.* (1991) TS model, as presented in Table 3. The estimates of biomass vary significantly with krill-orientation distribution, whereas the associated coefficients of variation remain similar. Demer and Conti (2005) emphasized that there is still significant uncertainty about krill orientation beneath survey vessels, and the temporal and spatial dependences. However, krill orientation is usually not accounted for when estimating empirical krill TS.

Conclusion

When applying the SDWBA model to estimate krill TS, it is necessary to adjust s.d. _{φ} vs. f , N , and L . Equations (8) and (9) are provided for this purpose. If the standard deviation of the phase s.d. _{φ_0} can be estimated empirically for a shape of krill $N_0 L_0$ for frequency f_0 , then the appropriate N and s.d. _{φ} can be determined to estimate TS vs. kL.

Table 3. Conversion factors for converting integrated echo energy to krill biomass B_0 for each cluster C1, C2, and C3 (Hewitt and Demer, 1991) resulting from the Greene *et al.* (1991) and SDWBA TS models; the associated krill biomass estimates; and their coefficients of variation (CV). Values were calculated with measured $c = 1456 \text{ m s}^{-1}$ (Demer, 2004), opposed to the nominal value of $c = 1500 \text{ m s}^{-1}$ used by Demer and Conti (2005). Consequently, the values here for Greene *et al.* (1991) and $N(15^\circ, 5^\circ)$ differ slightly from those in Demer and Conti (2005). Three clusters of krill-length distribution were identified by net-sampling for different portions of the CCAMLR 2000 survey area (Hewitt *et al.*, 2002). C1 is a narrow length distribution centred at 26 mm (small krill); C2 is a broad and somewhat bimodal length distribution peaking at 46 mm (mixed sizes); and C3 is a positively skewed length distribution centred at 52 mm (large krill).

TS model	Frequency (kHz)	Conversion factor			B_0 (Mt)	CV (%)
		C1	C2	C3		
Greene <i>et al.</i> (1991)	38	0.5163	0.4786	0.4661	29.4	9.3
	120	0.1636	0.1517	0.1477	44.1	11.5
	200	0.0981	0.0910	0.0886	44.8	15.7
SDWBA $N(11^\circ, 4^\circ)$	38	0.6275	1.1437	1.1925	65.67	11.0
	120	0.3844	0.7066	0.8787	189.3	10.6
	200	0.4069	0.8411	1.0548	342.7	12.5
SDWBA, C1 $N(9^\circ, 1^\circ)$; C2 $N(4^\circ, 2^\circ)$; and C3 $N(3^\circ, 1^\circ)$	38	0.9826	1.3313	0.8766	68.7	10.2
	120	0.5538	0.4788	0.5209	145.8	11.7
	200	0.5146	0.6880	0.9305	318.8	13.3
SDWBA $N(4^\circ, 2^\circ)$ C1, C2, and C3 weighted by survey area	38	1.2022	1.3313	0.9755	73.0	9.7
	120	0.2475	0.4788	0.6183	128.9	10.7
	200	0.2834	0.6880	0.9026	274.6	12.4
SDWBA $N(15^\circ, 5^\circ)$	38	2.5379	1.5189	1.3632	100.1	8.9
	120	0.2857	0.3882	0.4575	108.0	10.4
	200	0.2165	0.4109	0.5022	169.6	12.7

Using Equations (8) and (9), krill biomass in the Scotia Sea could be re-evaluated to nearly three times the previously reported biomass, but these new estimates depend greatly on the krill orientation used for the model. The study of this dependence goes beyond the aim of this work, but should be investigated further to provide better estimates of krill biomass. Using survey data, the krill-orientation distribution was estimated here to either $N(4^\circ, 2^\circ)$ or $N(11^\circ, 4^\circ)$ depending on the data being averaged per surveyed cluster area or krill catch demographics, respectively. Coefficients for the simplified version of the SDWBA model are also provided for both orientation distributions. One might also investigate whether there are differences in the orientation distributions of krill beneath different survey vessels and with survey speed.

Acknowledgements

We thank Kazuo Amakasu and Masahiko Furusawa, Tokyo University of Marine Science and Technology, for bringing this sensitivity of the SDWBA model to our attention, and two reviewers for their valued comments on an earlier draft of the manuscript.

References

- Chu, D., and Wiebe, P. H. 2005. Measurements of sound-speed and density contrasts of zooplankton in Antarctic waters. *ICES Journal of Marine Science*, 62: 818–831.
- Conti, S. G., Demer, D. A., and Brierley, A. S. 2005. Broadband-width sound scattering and absorption from krill (*Meganyctiphanes norvegica*), mysids (*Praunus flexuosus* and *Neomysis integer*) and shrimp (*Crangon crangon*). *ICES Journal of Marine Science*, 62: 956–965.
- Demer, D. A. 2004. An estimate of uncertainty in the CCAMLR 2000 acoustical estimate of krill biomass. *Deep-Sea Research II*, 51: 1237–1251.
- Demer, D. A., and Conti, S. G. 2003a. Reconciling theoretical versus empirical target strengths of krill; effects of phase variability on the distorted wave Born approximation. *ICES Journal of Marine Science*, 60: 429–434.
- Demer, D. A., and Conti, S. G. 2003b. Validation of the stochastic distorted-wave Born approximation model with broadbandwidth total target strength measurements of Antarctic krill. *ICES Journal of Marine Science*, 60: 625–635.
- Demer, D. A., and Conti, S. G. 2005. New target-strength model indicates more krill in the Southern Ocean. *ICES Journal of Marine Science*, 62: 25–32.
- Endo, Y. 1993. Orientation of Antarctic krill in an aquarium. *Nippon Suisan Gakkaishi*, 59: 465–468.
- Foote, K. G., Everson, I., Watkins, J. L., and Bone, D. G. 1990. Target strengths of Antarctic krill (*Euphausia superba*) at 38 and 120 kHz. *Journal of the Acoustical Society of America*, 87: 16–24.
- Greene, C. H., Stanton, T. K., Wiebe, P., and McClatchie, S. 1991. Acoustic estimates of Antarctic krill. *Nature*, 349: 110.
- Hewitt, R. P., and Demer, D. A. 1991. Krill abundance. *Nature*, 353: 310.
- Hewitt, R. P., Watkins, J. L., Naganobu, M., Tshernyshkov, P., Brierley, A. S., Demer, D. A., Kasatkina, S., Takao, Y., Goss, C., Malysenko, A., Brandon, M. A., Kawaguchi, S., Siegel, V., Trathan, P. N., Emery, J. H., Everson, I., and Miller, D. G. M. 2002. Setting a precautionary catch limit for Antarctic krill. *Oceanography*, 15(3): 26–33.
- Kils, U. 1981. The swimming behaviour, swimming performance and energy balance of Antarctic krill *Euphausia superba*. *BIOMASS Scientific Series*, 3. 122 pp.
- Martin-Traykovski, L. V., O'Driscoll, R. L., and McGehee, D. E. 1998. Effect of orientation on the broadband acoustic scattering of Antarctic krill (*Euphausia superba*): implications for inverting zooplankton spectral acoustic signatures for angle of orientation. *Journal of the Acoustical Society of America*, 104: 2121–2135.
- McGehee, D. E., O'Driscoll, R. L., and Martin-Traykovski, L. V. 1998. Effects of orientation on acoustic scattering from Antarctic krill at 120 kHz. *Deep-Sea Research II*, 45: 1273–1294.
- Morse, P. M., and Ingard, K. U. 1968. *Theoretical Acoustics*. Princeton University Press, Princeton, NJ. 927 pp.
- Pauly, T., and Penrose, J. D. 1998. Laboratory target-strength measurements of free-swimming Antarctic krill (*Euphausia superba*). *Journal of the Acoustical Society of America*, 103: 3268–3280.